DESIGN AND OPTIMISATION OF A NEW RTM COMPOSITE BICYCLE CRANK

M. Quaresimin[1], G. Meneghetti[2], G. Ronda[3] and F. Verardo[2]

[1] *Department of Management and Engineering, University of Padova*
Stradella San Nicola 3, Vicenza, 36100, Italy
[2] *Department of Mechanical Engineering, University of Padova*
Via Venezia 1, Padova, 35131, Italy
[3] *Ronda Europa SpA Via Vegri 83, Zanè - Vicenza, 36010, Italy*

SUMMARY: The paper presents the activities performed for the design and the optimisation of a new carbon fibre composite bicycle crank produced by using the RTM technology.
A prototype of the right crank was developed on the basis of a preliminary finite element model. Its flexural and torsional stiffness performances were evaluated and compared with those of top quality commercial cranks made of aluminium alloy or composite material.
The preliminary FE model was carefully calibrated after the evaluation of the elastic properties of the constituents materials and by means of suitable experimental tests.
Finally, by simulating the stiffness tests, a FE optimisation was performed with the aim to increase the specific stiffness and to investigate the influence, on the stiffness performances, of the elastic properties and lay-up of the materials the crank is made of.

KEYWORDS: Bicycle crank, RTM, Design, Optimisation

INTRODUCTION

The need of lightness and stiffness in the bicycle industry products has been continuously increasing in the last years.
A possible solution to satisfy these requirements is the use of advanced composite materials, because of their high stiffness and strength to weight ratios. Nevertheless, the major drawback of the composite components is the production cost, frequently much higher with respect to products made of commonly used metallic materials such as steel and light alloy.
The Resin Transfer Moulding (RTM) seems to be suitable to overcome this limitation; this production technology, strongly improved in the last years, allows in fact the industrial production of high performance composite components at acceptable costs. RTM represents a good cost-saving alternative to the traditional labour-intensive bag moulding process with much higher production rates and a production cycle easier to be industrialised. Moreover, it is possible to encapsulate metal inserts in the moulded parts or a foam core between the top and the bottom pre-forms of a hollow part, adding stiffness to the structure and allowing to mould complex three dimensional shapes.

On this basis it was decided to develop a new bicycle crank made in carbon fibre/epoxy composite by using the RTM technology. This paper deals with a synthesis of the activities performed for the design, development and optimisation of the new composite crank.
This task was accomplished according to an integrated design procedure, including material property evaluation, prototype testing and structural FEM optimisation; this integrated procedure, successfully applied in the design and optimisation of racing motorcycles components [1, 2], turned out to be the most effective solution to match the lightness and stiffness requirements.

The experimental and numerical activities carried out during the design process can be summarised as follow:

- design and production of the first prototype of the right composite crank;
- material property evaluation (composite material laminates, epoxy and polyurethanic foams, aluminium-composite bonded joints);
- flexural and flexural/torsional stiffness tests on the cranks;
- development and calibration of the FE model for the right composite crank;
- FE flexural/torsional stiffness optimisation;

First prototype development

After the definition of the global geometry according to the Standards in force [3,4] and some style requirements, the first crank prototype was built as a sandwich structure, by using carbon/epoxy laminates and structural foam.
The pre-forms were made of T800 carbon fibre plain weave fabric layered with a $[0,45]_n$ lay-up and impregnated with an Araldit 5052 LY (Ciba-Geigy) epoxy resin system. For the foam core an epoxy structural foam BIRESIN VP680 was used.
The connections at the bottom bracket axle and at the pedal spindle were obtained by means of two cylindrical aluminium alloy inserts positioned in the crank and bonded after moulding by using an Araldit 420A/B Ciba-Geigy epoxy adhesive.
The first crank prototype is presented in the photograph of figure 1: it is easy to see that the main geometrical difference with respect to a traditional aluminium crank is the palmate zone bracing the spider spokes, which was inserted to increase the crank stiffness and to simplify the production.

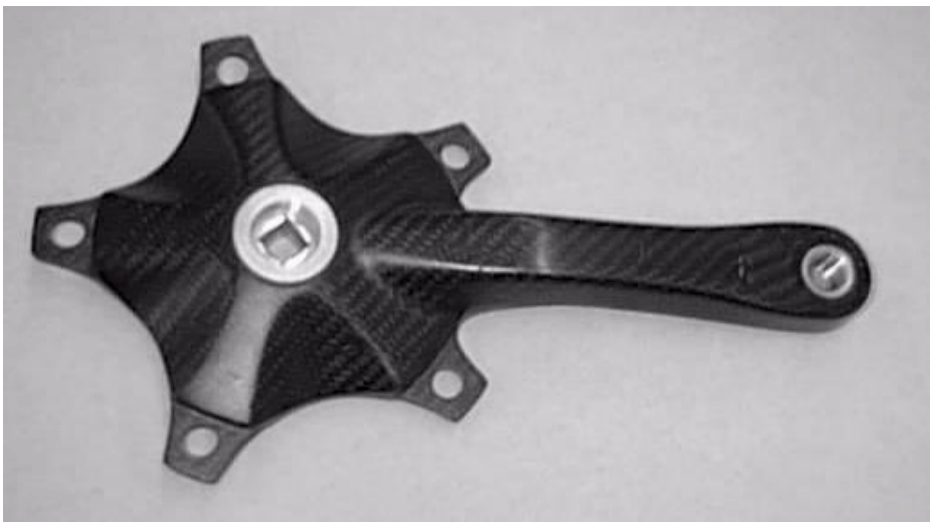

Fig. 1: The first prototype of the right crank

Material property evaluation

All the materials used in the crank prototype manufacturing were carefully tested with the aim to obtain the elastic and strength properties needed for an accurate FE simulation of the crank structural behaviour.
In particular, the mechanical and physical properties of the following materials were evaluated:

- composite laminate, T800 carbon fibre plain weave fabric/Araldit LY 5052 (Ciba-Geigy) epoxy resin system, ≈50 % nominal fibre volume fraction;
- epoxy structural foam BIRESIN VP680;
- polyurethanic structural foam AIREX;
- Araldit 420A/B (Ciba-Geigy) epoxy adhesive;
- Araldit 2011 (Ciba-Geigy) epoxy adhesive;
- 7075-T6 aluminium alloy.

In order to avoid the influence of the production process in the materials properties, the laminate were moulded by using the same process applied for the crank manufacturing. The specimens were cut by using a diamond saw and tested according to the ASTM D3039-76 Standard [5].
The elastic properties of the epoxy foams and aluminium alloy were evaluated in tension by using strain gauged dog-bone specimens of suitable dimensions, while for the characterisation of the adhesives, double lap composite-aluminium specimens were used and the static and fatigue shear strength were evaluated. Table 1 summarises the results of the material characterisation.

Table 1: Average properties of the materials used in the crank manufacturing

Composite laminate	E_L [MPa]	E_T [MPa]	ν_{LT}	G_{LT} [MPa]	σ_L [MPa]	σ_T [MPa]	τ_{LT} [MPa]
T800/5052	61500	61500	0.062	3900	760	760	120
Isotropic material	E [MPa]	ν	ρ [kg/m^3]	τ_r [MPa]	$\Delta\tau_a$ [MPa]	k	
BIRESIN VP680	780	0.297	472	-	-		
AIREX	280	0.281	218		-		
7075-T6	71700	0.33	2800	-	-		
Araldit 420A/B	-	-	-	34	-	-	
Araldit 2011	-	-	-	15	2.9	7.7	

[subscript L indicates the direction parallel to the fabric warp, the subscript T indicates the transverse direction. $\Delta\tau_a$ and k: stress range ($2\cdot10^6$ cycles and 50% p. of s.) and inverse slope of the bonded joints Wöhler curve, respectively]

Experimental stiffness tests

The main design requirement of a bicycle crank can be considered, as said above, its stiffness, being the expected structural performances strongly related to this parameter; therefore it was decided to develop a flexible testing device for evaluating the crank stiffness under different load cases which simulate as much as possible the in-service loading conditions. A global view of the testing device, developed also accounting for the recommendations of the present Standards on bicycles [3,4], is presented in figure 2.
The testing device is shown fixed to a universal testing bench with movable hydraulic actuators equipped with load cells and LVDT displacement transducers. The device is made, mainly, of bolted steel plates and allows the execution of both static and fatigue tests on single crank or on the complete crank set assembly.

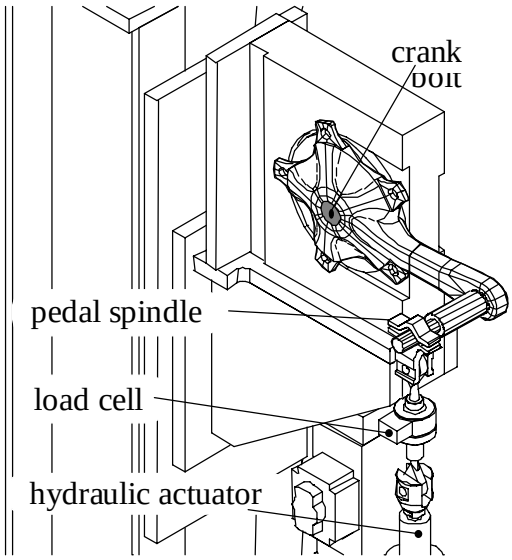

Fig. 2: The stiffness testing device

The stiffness tests were oriented to different purposes like the evaluation and the comparison of the structural performances of different cranks, the FE model calibration and the accomplishment of the Standard requirements. Accordingly, several test set-ups were defined.

However, all the test set-ups presented common features: an isostatic constraint configuration was chosen for a more reliable simulation in the FE analyses and they are representative of different in-service loading conditions. Moreover the stiffness parameters resulting from each test set-up measure the structural contribution of the different parts of the crank, therefore giving useful information during the design development.

In the first test set-up, from now on referred to as FS (fixed spindle) test, the crank is rigidly bolted to a spindle, simulating the bottom bracket spindle, welded on a circular flange. The flange is then bolted to the testing device therefore eliminating the rotational degree of freedom typical of the bottom bracket axle.

The test procedure, from a practical point of view, consists in the incremental application of a vertical load F_V at the pedal spindle, simulated by a steel bar, and in the measurement of the resulting crank deflections d_1 and d_2, as shown in figure 3-a.

The flexural and torsional stiffness, defined by the equations (1) and (2), are evaluated by a linear best fit of the experimental results of at least three repeated tests.

$$K_F = \frac{F_V}{d_1} \quad (1) \qquad K_T = \frac{F_V \cdot b}{|d_2 - d_1| / b} \quad (2) \qquad K_L = \frac{F_H}{d_3} \quad (3)$$

Equations for the flexural, torsional and lateral stiffness evaluation

In the FS test configuration, the crank behaves as a cantilever beam and the resulting global stiffness is due to the contribution of both the crank shank stiffness and the stiffness of the bonded joint between the aluminium insert and the composite part of the crank. This test set-up is very simple and useful for a quick comparison of the performances of different cranks.

A second test set-up (FSC, free spindle and chain) was defined, which is more representative of the crank in-service behaviour: the crank is connected by means of the crank bolt to the axle of the bottom bracket**,** housed in the testing rig and the rotational degree of freedom is eliminated by fixing the upper spoke to the rear plate of the testing device with a short piece of chain (figure 3-b). The test procedure and the evaluation of the crank stiffness coincide with those reported above for the FS test set-up, with the difference that the FSC test can be performed only on right cranks. This set-up allows the evaluation of the spoke contribution to the crank stiffness, as compared with the FS test set-up.

The last test set-up, referred to as FSL test (fixed spindle, lateral), presents the same constraint configuration of the FS test set-up with the only change of the direction of the load application from vertical (F_V) to horizontal (F_H) and, consequently, measuring the horizontal displacements d_3 (figure 3-c). The lateral flexural stiffness can be evaluated by using the equation (3). In this last case, the stiffness results are mainly related to the crank shank behaviour with only a very slight influence of the aluminium-composite joint stiffness.

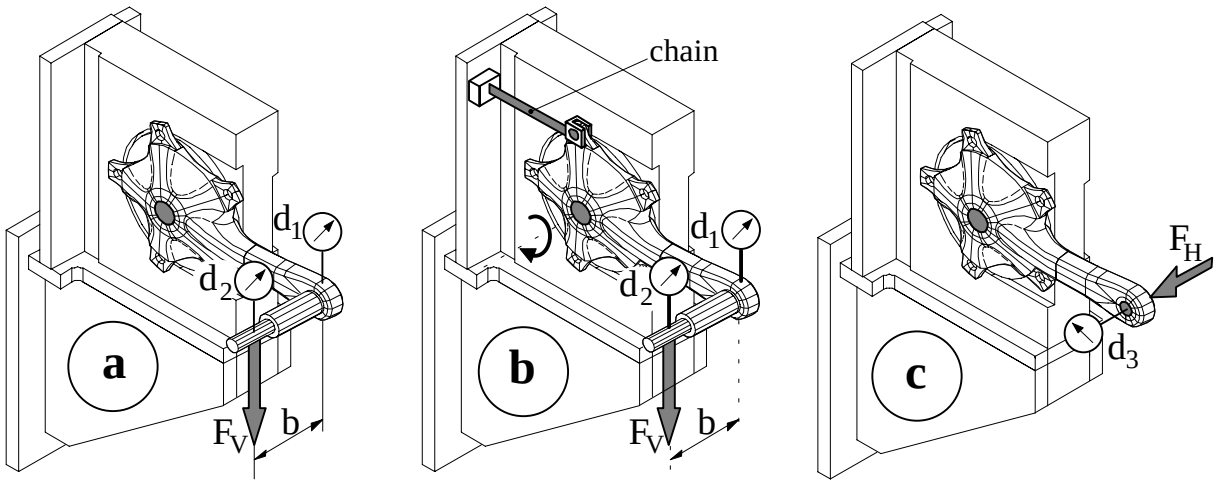

Fig. 3: Set-up for the stiffness tests. (a): FS test (fixed spindle), (b): FSC test (free spindle and chain), (c): FSL test (fixed spindle, lateral).

During the stiffness tests with the different set-ups, the constraint compliance was also evaluated and the results were used for the correction of the crank stiffness values: the measured displacements d_1, d_2 and d_3 were respectively reduced to correctly account for the rigid body motion of the crank during the tests. In particular, the flexural and torsional compliance of the fixed steel spindle and of the bottom bracket spindle were measured as well as the axial compliance of the chain. The evaluation of the constraint compliance resulted very useful for the subsequent comparison between experimental and numerical stiffness results for the calibration of the crank FE model.

In the preliminary phase of the design process, two types of top quality commercial right aluminium alloy cranks and one commercial composite right crank were tested and the results were compared with those obtained for the first prototype of the right crank. The aluminium cranks, referred to as ALU 1 and ALU 2, are forged, while the commercial composite crank, referred to as COMPO, is produced with the traditional vacuum bag autoclave moulding. The new under development RTM prototype will be referred to as KARBO.

For a quick comparison of the stiffness performances of the different cranks, table 2 summarises the stiffness test results, reported without the correction which accounts for the constraint compliance. The crank weights are also listed.

Table 2: Stiffness test results for the different tests and cranks

CRANK	Weight [g]	K_F (FS) [N/mm]	K_T (FS) [Nm/rad]	K_F (FSC) [N/mm]	K_T (FSC) [Nm/rad]	K_L (FSL) [N/mm]
KARBO	242	207	1283	350	1379	153
ALU 1	294	272	1861	275	2422	181
ALU 2	260	247	1504	240	1580	134
COMPO	241	186	2060	356	2272	235

From table 2 we can immediately observe the low values of both flexural and torsional stiffness of the new prototype in the FS test: this can be due to the relatively low stiffness of the bonded aluminium composite joint and to the non-optimised lay-up, particularly with respect to the torsional stiffness. As a further confirmation, the torsional stiffness remains too low even in the FSC test set-up; on the other hand, in this case, the flexural stiffness of the KARBO crank is very high, suggesting a strong contribution, to the overall crank stiffness, of spokes and palmate area. Finally, in the lateral stiffness test (FSL) the flexural stiffness K_L assumes acceptable value; being K_L only slightly influenced by the bonded joint stiffness, it

can be concluded that this joint has instead strong influence in the flexural stiffness of the FS test. However, it should also be noted the lower weight of the KARBO crank with respect to those made of aluminium alloy. Therefore, by rearranging the results in terms of specific properties lower differences can be expected. As an example, by comparing the flexural stiffness in the FS test set-up, the difference between ALU 1 and KARBO cranks is about 25% in the absolute stiffness dropping to 8% only in terms of specific stiffness. In spite of this, the improvements of the absolute torsional and flexural stiffness of the KARBO prototype were considered as primary requirements during the structural FE optimisation.

FE modelling

The FE model of the crank was build by using the ANSYS 5.3 FE code on the basis of the 3D crank geometry generated with PRO/Engineering.
As above mentioned, the crank was made as a sandwich structure with an external, continuous skin of composite laminate and a structural foam core. Previous experiences on box sandwich structure FE modelling [6], suggested that the most effective way to simulate the behaviour of these structures is the use of solid elements both for the isotropic core and the orthotropic skin.

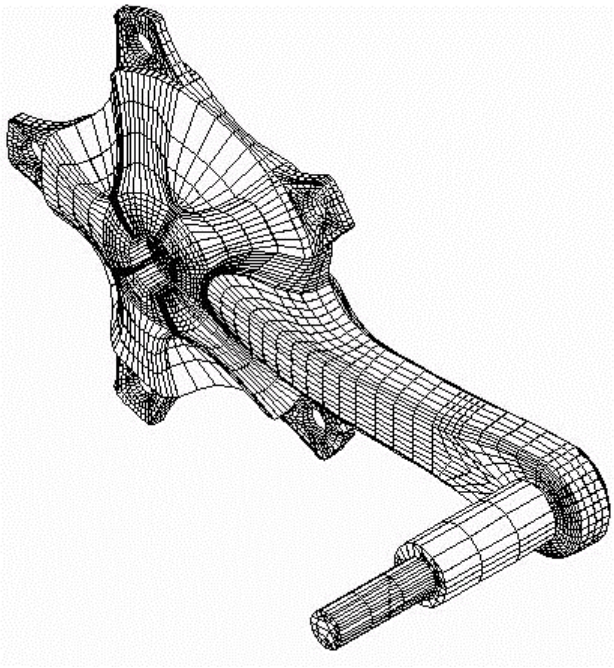

Fig. 4: FE model of the right prototype crank

The greater time needed for the model definition and the increased complexity of the model itself are largely counterbalanced by the greater accuracy of the results in terms of displacements and local strains.
The layered solid elements (SOLID46) of ANSYS require, however, a great care in the construction of the model volumes in order to obtain rightly oriented element frames of reference in the subsequent mapped meshing. Moreover, this approach together with the complexity of the crank geometry brought sometimes to non-uniform size elements.
The final model of the complete crank is presented in figure 4; for a more realistic simulation of the applied loading condition it was decided to model the pedal spindle too. The external composite skin of the crank was modelled by using 4568 orthotropic 8-nodes layered elements (SOLID 46) while for structural foam, metallic inserts and adhesive layers 11608 isotropic 8-nodes elements (SOLID 45) were used.
Hence, the final crank model consisted of 16176 solid elements for a total number of 20447 nodes and 60708 active DOFs; the size of the FE model file (FILE.DB) resulted approximately of 45 Mb, the results file (FILE.RST) of 40 Mb and the temporary files required about 670 Mb with the Frontal solver and about 250 Mb with the PCG solver. The CPU time needed for a linear elastic solution was about 15 minutes on a workstation SUN Ultra Sparc II-1170 (170 MHz CPU- 128 Mb RAM memory).
For a more clear understanding of some of the FE model features, figure 5 shows two enlargements of the model’s mesh: it is easy to see the presence of the foam core inside the model, the mesh density and the solutions adopted to model the zones with highly distorted geometry.

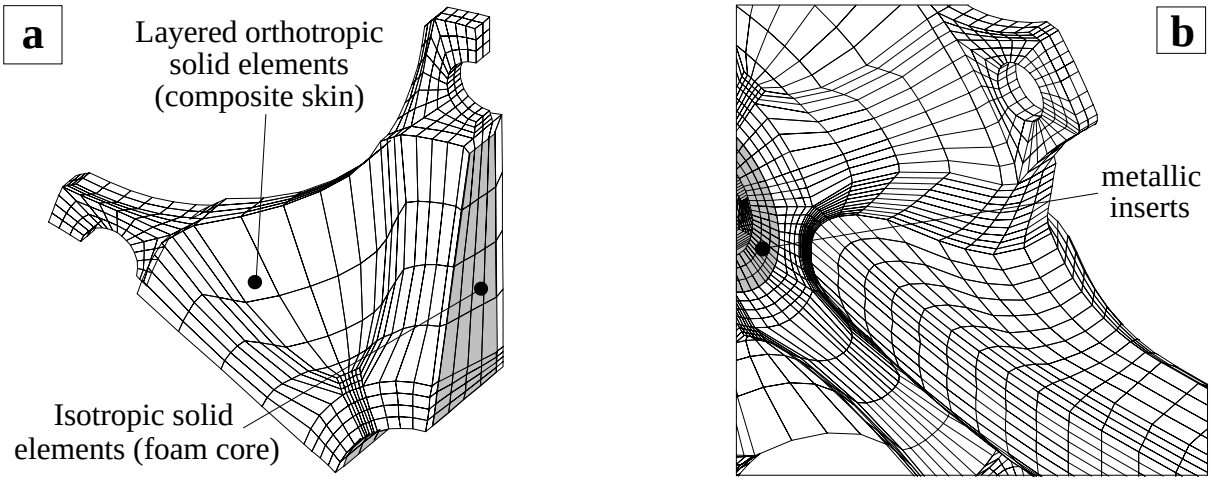

Fig. 5: Enlarged views of the mesh of some crank sections; (a) mesh of the palmate zone between two spokes and foam core, (b) mesh of the connecting volume between the spoke palmate zone and the crank shank

During the preliminary analyses, the stiffness response of the crank FE model turned out to be very sensitive to the presence of the adhesive layer between the crank composite body and the metallic inserts; hence, this layer was introduced in the crank model and modelled, as said above, with isotropic solid elements; in spite of the very low thickness of these elements, a more precise simulation of the crank stiffness behaviour was obtained.
However, the adopted modelling solution resulted unsuitable for the correct estimation of the stress field inside the adhesive layer due to both the very thin thickness of the elements, if compared with the other dimensions, and the very difficult evaluation of the adhesive elastic properties. The uncertainty in the adhesive elastic properties did not affect, on the other hand, the stiffness response as we verified for a quite wide range of variation.
The final refined crank FE model was then calibrated by simulating the experimental stiffness tests previously made; the model calibration was done on the basis of the experimental results after the correction accounting for the real constraint compliance. In spite of this a careful adjustment of the numerical loading and constraint conditions was needed for a realistic simulation of the crank structural behaviour.
Table 3 compares the experimental and numerical stiffness results of the different test set-ups and reports also the errors in the numerical estimation.

Table 3: Comparison of numerical and experimental stiffness results *

Test Set-Up	K_F(FEM) [N/mm]	K_F(Exp.) [N/mm]	Error (%)	K_T(FEM) [Nm/rad]	K_T(Exp.) [Nm/rad]	Error (%)	K_L(FEM) [N/mm]	K_L(Exp.) [N/mm]	Error (%)
FS	361	288	20	1359	1436	-6	-	-	-
FSC	364	358	2	1341	1107	17	-	-	-
FSL	-	-	-	-	-	-	218	210	4

(*: after the correction accounting for the constraint compliance)

Considering the complexity of the structure, a reasonably good agreement was found between numerical and experimental results.
The low errors (4-5%) in the lateral stiffness evaluation suggest a good reliability of the FEM model results. However, the greater errors in the FS and FSC test simulation, and also the fact that the torsional and the flexural stiffness are estimated with errors which depend on the type of test indicate that the presence of the adhesive layer, simulated with very thin elements, and also the constraint modelling could probably still have some influence on the results.

Stiffness optimisation

The optimisation phase was mainly oriented to improve the torsional and flexural stiffness properties of the KARBO prototype, being these parameters lower, in absolute terms, with respect to the other commercial cranks.
The stiffness tests were numerically simulated and the influence of the following parameters were analysed:

- skin laminate lay-up;
- fibre and foam elastic properties;

The influence of skin lay-up and fibre properties was investigated by means of the FE models listed in table 4. For the A to F models, only the skin lay-up was changed with respect to the $[0,45]_n$ lay-up of the first prototype. The G to L models simulated, instead, cranks made of materials with different elastic properties, considering as alternative material an high modulus M46J twill 2-2 carbon fabric always impregnated with Araldit 5052 LY epoxy system (E_L= E_T= 122000 MPa, G_{LT}= 6800 MPa, ν_{LT}= 0.06). Table 4 indicates the portion of the crank where the material properties were changed with respect to those of the first prototype.

Table 4: Features of the FE crank models analysed

Model	lay-up	Model	Modified skin zones
A	[0,30,60,30,0,30,60,30,0]	**G**	rear skin
B	[0,45,60,45,0,45,60,45,0]	**H**	front skin
C	[0,30,45,60,45,60,45,30,0]	**I**	complete skin
D	[0,30,45,30,0,30,45,30,0]	**L**	crank shank
E	[0,45,60,45,0,45,60,45,0]		
F	[0,15,45,55,45,55,45,15,0]		

Another interesting analysis could be the investigation of the effects of the skin thickness variations on the stiffness performances. Unfortunately, being the skin modelled with solid elements, this analysis would have required the solid models to be completely rebuilt. However, a rough prediction of the thickness influence can be done by considering that the increase in the elastic laminate properties approximately corresponds to the same increase in the thickness, by keeping the elastic properties unchanged. Therefore the results obtained from the G to L models are meant to be regarded as the effect of both material elastic properties or thickness variations.
Figure 6 presents a synthesis of the results obtained by simulating the different stiffness test set-ups with the FE models listed in table 4. The results are presented in terms of percentage variation with respect to the first prototype properties.
It is clearly evident that by acting on the skin lay-up only (models A to F) an increase in the torsional stiffness is normally related to a decrease in the flexural stiffness. Improvement up to 20% in both FS and FSC torsional stiffness are easy to be obtained provided that a reduction of less than 10% is accepted in the flexural stiffness. The situation changes completely if we consider the results of the G to L models. In fact, by increasing the elastic material properties, even if in some zones of the crank only, considerable improvements in all the stiffness parameters can be achieved. The results obtained for the I and L models are worth to be discussed more in detail: doubling the elastic properties of the complete crank skin gives only an average increase of 50% in stiffness while by modifying the properties only of the crank shank an increase greater than 40% in both Fs and FSC torsional stiffness can be obtained.

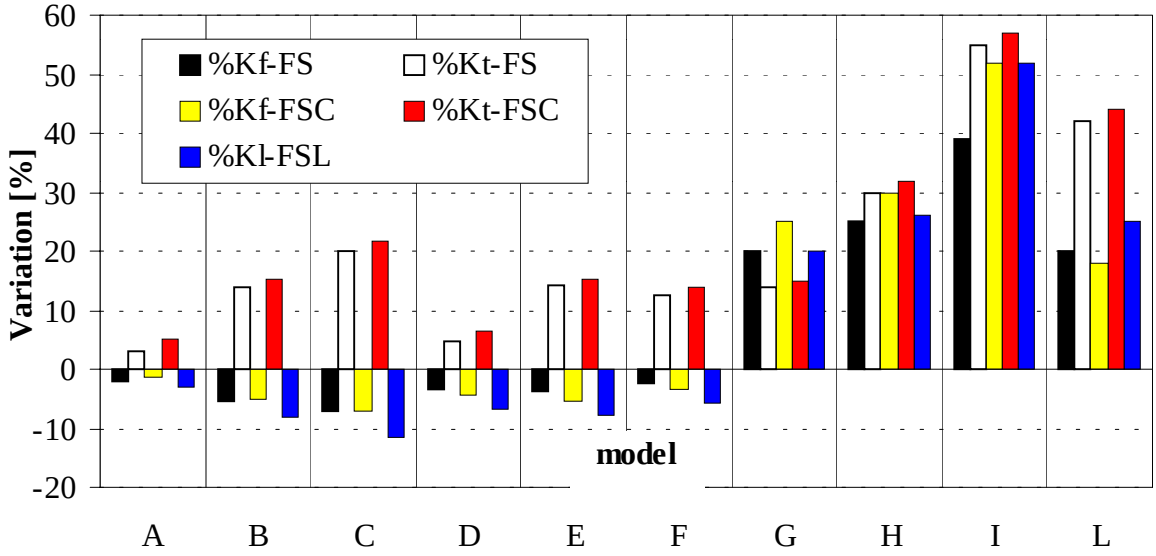

Fig. 6: Variation of the stiffness properties, with respect to the first prototype, of the crank FE models listed in table 4.

The A to L models refer substantially to cranks where no weight changes took place. A quite simple way to reduce the crank weight, without geometry and skin modifications, is by acting on the core foam density. To analyse the influence of the foam properties on the structural crank performances, a simplified linear relationship was assumed between the density and the tensile modulus of the structural core foam [7,8] and therefore the foam density changes were numerically simulated by a change of the foam elastic properties. A reduction in the crank weight of 7%, 14% and 18%, respectively, was estimated for the three analysed conditions with respect to the first prototype, having a foam tensile modulus E= 780 MPa.
The changes in the foam modulus brought to a consistent reduction in the crank stiffness properties, up to 20%. However, re-elaborating the results in terms of specific properties no reductions or only slight variations were found, as reported in Figure 7.

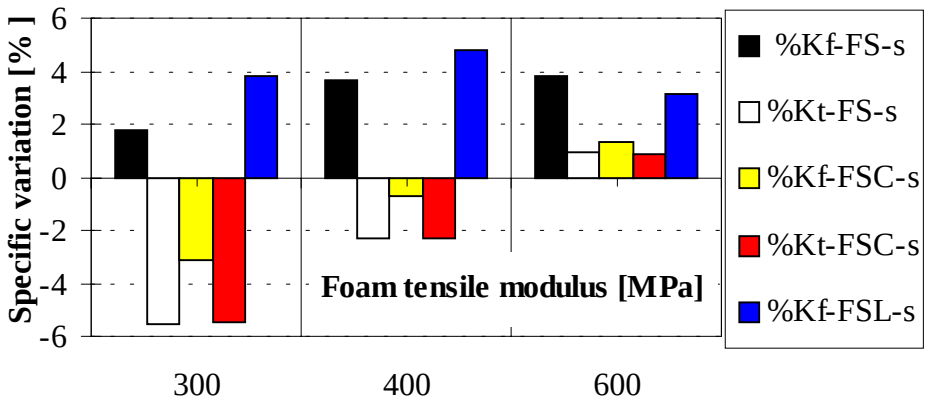

Fig. 7: Influence of the foam tensile modulus on the crank specific stiffness properties

Ongoing activities and further developments

The bonded aluminium composite joints turned out to be the weakest point of the new crank, particularly with respect to the fatigue behaviour. To overcome this limit a new design solution for the element of connection with the bottom bracket spindle is under analysis. Furthermore, an experimental test programme is being planned concerning the acquisition of the in service-loads on the cranks, for a reliable fatigue analysis.

CONCLUSIONS

The experimental and numerical activities done for the design, development and optimisation of a new composite bicycle crank, produced by using the RTM technology, have been presented.

After a preliminary design a first prototype was manufactured and its structural properties were compared with those of commercial cranks, by means of flexural and torsional stiffness tests simulating the in-service loading conditions.

A FE model of the crank was also developed, allowing the simulation of the crank behaviour and the optimisation of its structural performances.

Significant improvements, up to 20%, in the torsional stiffness were obtained by acting on the skin laminate lay-up only. On the other hand, high modulus M46J material was used instead of high strength T800 material to increase the flexural stiffness.

The FE simulation also highlighted a strong contribution of the crank shank stiffness to the overall torsional stiffness, while the properties of the palmate area bracing the spider spokes influenced mainly the flexural stiffness performances.

Finally, the crank behaviour turned out to be quite sensitive to the foam core properties: by modifying the foam density, considerable weight reductions were achieved with only slight variations in the specific stiffness properties.

REFERENCES

1. Meneghetti, G., Quaresimin, M. and Fabbri, L., “Optimisation of the Structural Performances of Racing Motorcycle Components”, *Proceedings of the Power Two Wheels International Conference*, Pisa , Italy, December 14-15, 1998, pp.113-122.
2. Lazzarin, P., Meneghetti, G., Petrone, N. and Quaresimin, M., “Structural Analysis of a Racing Motorcycle Composite Swing Arm”, *Proceedings of the Second International Seminar “Experimental Techniques and Design in Composite Materials”*, Sheffield, UK, September, 1994, M.S. Found Editor, Sheffield Academic Press, 1995, pp.350-364.
3. UNI 10395-1994: “Bicycles-Safety requirements” UNI, Milan, Italy, October 1994, (in Italian).
4. ISO 4210:1996E: “Cycles-Safety requirements for bicycles” Fourth edition 1996-11-01
5. ASTM D3039-76, "*Standard Test Method for Tensile Properties of Fibre-Resin Composites*". American Society for Testing and Materials - Philadelphia, USA, 1976.
6. Meneghetti, G. and Quaresimin, M., “FE Modelling of Box Sandwich Structures” *Internal Report C.M. 21-97,* Department of Mechanical Engineering, University of Padova, 1997.
7. Lubin, G., *Handbook of Composites*, Van Nostrand Reinhold, New York, USA, 1981
8. Caprino, G. and Teti, R., *Sandwich Structures Handbook*, Ed.Il Prato, Padova, Italy, 1989.